Making corrections to your proof

Please follow these instructions to mark changes or add notes to your proof. You can use Adobe Acrobat Reader (download the most recent version from **https://get.adobe.com**) or an open source PDF annotator.

For Adobe Reader, the tools you need to use are contained in **Annotations** in the **Comment** toolbar. You can also right-click on the text for several options. The most useful tools have been highlighted here. If you cannot make the desired change with the tools, please insert a sticky note describing the correction.

Please ensure all changes are visible via the 'Comments List' in the annotated PDF so that your corrections are not missed.

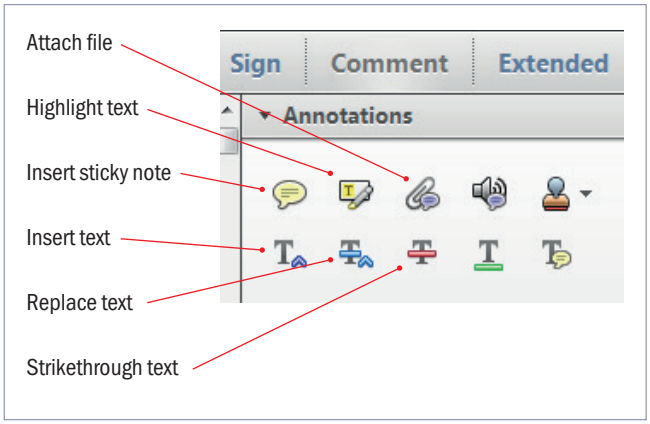

Do not attempt to directly edit the PDF file as changes will not be visible.

Replacing text

To replace text, highlight what you want to change then press the replace text icon, or right-click and press 'Add Note to Replace Text', then insert your text in the pop up box. Highlight the text and right click to style in bold, italic, superscript or subscript.

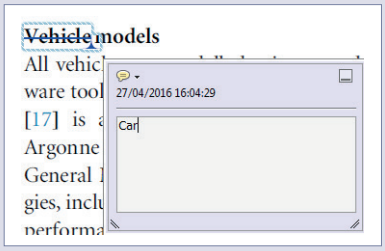

Inserting text

Place your cursor where you want to insert text, then press the insert text icon, or right-click and press 'Insert Text at Cursor', then insert your text in the pop up box. Highlight the text and right click to style in bold, italic, superscript or subscript.

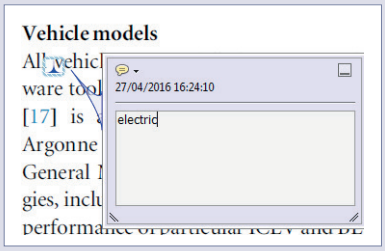

Deleting text

To delete text, highlight what you want to remove then press the strikethrough icon, or right-click and press 'Strikethrough Text'.

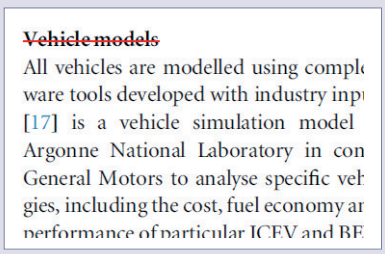

Highlighting text

To highlight text, with the cursor highlight the selected text then press the highlight text icon, or right-click and press 'Highlight text'. If you double click on this highlighted text you can add a comment.

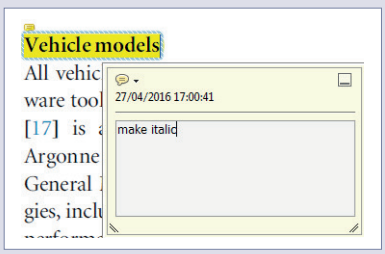

QUERY FORM

JOURNAL: Nanotechnology

AUTHOR: K C Yang *et al*

TITLE: Highly oxidation-resistant silver nanowires by C_xF_y polymers using plasma treatment

ARTICLE ID: nanoab114c

The layout of this article has not yet been finalized. Therefore this proof may contain columns that are not fully balanced/ matched or overlapping text in inline equations; these issues will be resolved once the final corrections have been incorporated.

Please check that the **names of all authors as displayed in the proof are correct**, and that all **authors are linked to the correct affiliations**. Please also confirm that the correct corresponding author has been indicated. **Note that this is your last opportunity to review and amend this information before your article is published**.

If an explicit acknowledgment of funding is required, please ensure that it is indicated in your article. If you already have an Acknowledgments section, please check that the information there is complete and correct.

Note that the supplementary data associated with your article will be hosted as supplied, and will not be processed by us. If you wish to supply new files, please send them along with your proof corrections.

SQ1
Please be aware that the colour figures in this article will only appear in colour in the online version. If you require colour in the printed journal and have not previously arranged it, please contact the Production Editor now.

We have been provided with ORCID iDs for the authors as below. Please confirm whether the numbers are correct.
Geun Young Yeom 0000-0001-6603-2193

APP Template V1.70 Article id: nanoab114c Typesetter: MPS Date received by MPS: 21/03/2019 PE: MAC007654 CE: LE:

IOP Publishing Nanotechnology

Nanotechnology **00** (2019) 000000 (10pp)

Highly oxidation-resistant silver nanowires by C_xF_y polymers using plasma treatment

Kyung Chae Yang, Da In Sung, Ye Ji Shin and Geun Young Yeom

School of Advanced Materials Science and Engineering, Sungkyunkwan University, 2066, Seobu-ro, Suwon, 16419, Republic of Korea

E-mail: gyyeom@skku.edu

Received 31 October 2018, revised 28 February 2019
Accepted for publication 20 March 2019
Published DD MM 2019

Abstract

We demonstrate plasma-treated AgNWs as flexible transparent electrode materials with enhanced long-term stability against oxidation even in a high humidity environment (80% humidity, 20 °C). Through a simple fluorocarbon (C_4F_8 or C_4F_6) plasma treatment method, a C_xF_y protective polymer was sufficiently cross-linked and attached on the surface of the AgNWs strongly and uniformly. Even though C_4F_8 and C_4F_6 activate differently on the AgNW surface due to the different dissociated radicals formed in the plasma, it was found that the C_xF_y protective polymers obtained by both chemicals work similarly as a protective layer for transparent conductive electrodes; a nearly constant sheet resistance ratio (R_s/R_o) of 1.6 was found for AgNWs treated with C_4F_8 and C_4F_6 plasmas, while the AgNWs without the plasma treatment exhibited a ratio of 176.2 after 36 d in a harsh environment. It is believed that the fluorocarbon plasma treatment can be used as a key method for ensuring long-term oxidation stability in numerous electronic applications including flexible solar cells utilizing various types of metallic nanowires.

Supplementary material for this article is available online

Keywords: silver nanowire, transparent electrode, plasma treatment, oxidation resistive, hexafluoro-1,3-butadiene, octafluorocyclobutane, plasma polymers

SQ1 (Some figures may appear in colour only in the online journal)

1. Introduction

Transparent conductive materials, which make electrical contact with the active layer and provide a pathway for incident light, are a vital component of modern optoelectronic devices such as solar cells, light-emitting diodes (LEDs), and touch panels [1–4]. Traditionally, indium tin oxide (ITO) has been widely used in various types of transparent electrodes for optoelectronic devices because of its excellent optical transmittance (~90% at 550 nm) and low sheet resistance (~20 Ω sq^{-1}) [5, 6]. However, ITO thin films are too brittle to be used for flexible applications, require high deposition temperatures, and are expensive to produce [7]. Among several alternative materials, metal nanowires (NWs), such as silver nanowires (AgNWs), are attractive alternatives to conventional ITO films and a promising transparent electrode material [8, 9]. Randomly distributed AgNWs have already shown good optical transparency, electrical performance close to that of ITO, and good flexibility [10]. However, metal nanoscale networks such as AgNWs, copper NWs, and aluminum NWs have low resistance to oxidation and low stability in harsh environments, which can cause performance degradation and device failure [11–15]. The ease of oxidation and atmospheric corrosion impedes practical applications of AgNWs by dramatically reducing their conductivity [16, 17]. The presence of surface oxides on metal networks with nanoscale diameter has an especially severe impact due to the substantial increase in surface area, causing increases in the sheet resistance and haziness. This decreases the electrical conductivity of NW-based transparent electrodes and negatively impacts the overall device performance [18, 19]. In the case of solar cells with AgNWs as the top transparent electrode, it is known that the cell characteristics are seriously affected by the environment surrounding the solar cells due to

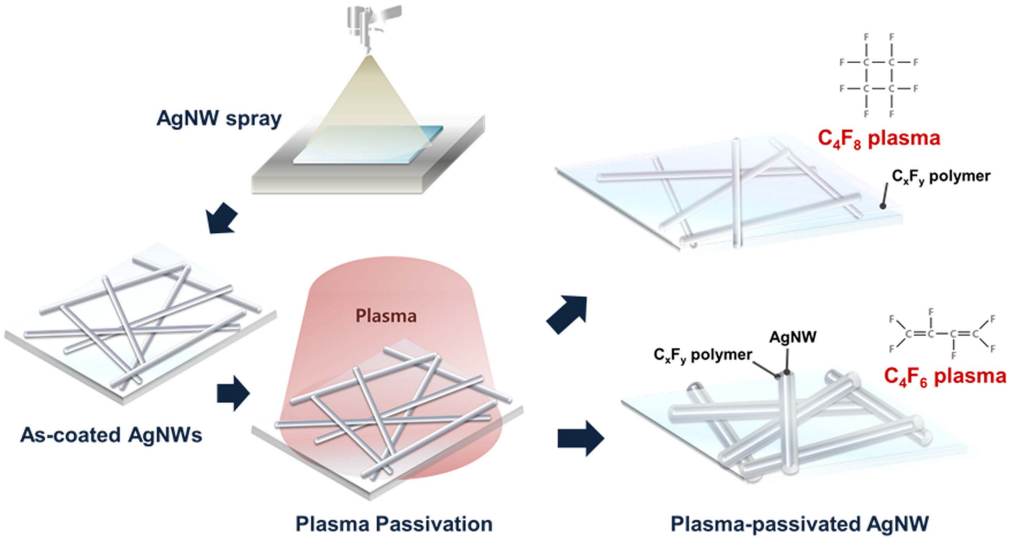

Figure 1. Schematic illustration of the spray coating of AgNWs onto glass substrates and plasma treatments using a C_4F_6 plasma and a C_4F_8 plasma.

the formation of Ag_2O or Ag_2S on the AgNW surface [20–22]. In this regard, one of the key issues facing high-performance AgNWs is the prevention of undesirable changes in the properties of the AgNWs and the maintenance of their electrical properties under ambient conditions [23, 24].

In order to improve the oxidation resistance and long-term stability of AgNWs, several approaches have been proposed to prevent the AgNW surfaces from being exposed to ambient conditions [25–28]. To maintain their optical transparency and good electrical conductivity, many researchers are investigating hybrid AgNW-based transparent conductive electrodes wrapped by the polymer polyvinylpyrrolidone, graphene, reduced graphene oxide, or other materials. Moreover, the coating of AgNWs with transparent materials such as aluminum-doped zinc oxide (AZO) or ZnO using low-temperature deposition processes, such as sputtering or atomic layer deposition, has recently been investigated [29–33].

Plasmas have been used in various processes such as surface treatments, etching, and deposition in order to dissociate the gases, increase the reactivity of the gases by forming radicals, and to modify the material surfaces. In particular, fluorocarbon plasmas have been used to etch silicon-based semiconductor materials and also to polymerize material surfaces. By dissociation of the stable fluorocarbon gas and recombination of the dissociated and unsaturated fluorocarbon radicals on the surface, a dense and uniform fluorocarbon layer is known to be formed on the surface of the material. As one of the methods for controlling the long-term oxidation stability of AgNWs, plasma processing can be an obvious alternative for coating oxidation-resistant materials onto NWs because it is easily applicable to commercial manufacturing due to its high reliability, uniform and large-area processing, and high processing rate. In fact, various plasma treatments on various NWs have been previously investigated for controlling the work function and removing surfactant materials on NWs, among other uses [34–39].

In the present work, we demonstrate the formation of oxidation-resistant, high-quality AgNW networks by treating the AgNW surface with plasmas. Specifically, C_xF_y polymers were introduced to protect AgNWs from oxidation, which is critically important for maintaining low sheet resistance even under ambient conditions. By forming a dense and transparent polymer layer on the AgNW surface, the AgNW surface could be successfully protected against oxygen and moisture in the environment while maintaining optical transmittance and without using expensive materials and processes. It is believed that the plasma polymerization method investigated in this study can be applied to other metal NWs and has significant potential as an easy, fast, uniform, and large-area method.

2. Experimental section

The AgNWs used in this study were supplied by Nanopyxis with a diameter and length of ~20 nm and ~60 μm, respectively, and were prepared in a solution diluted with isopropyl alcohol (IPA, 1 wt%). The solution was further diluted with one part of AgNW solution to nine parts of IPA (Duksan Pure Chemicals). Prior to spraying the AgNW solution onto glass substrates, the substrates were ultrasonically cleaned in acetone, alcohol, and deionized water for 15 min each and were then blown dry. The AgNWs were sprayed uniformly using a spray gun (Sparmax-GP 35) onto 25 mm × 25 mm cleaned glass substrates attached to an *X*–*Y* stage (30 cm × 30 cm) while the stage was heated to about 50 °C to remove the solvent easily.

Figure 1 shows a schematic diagram of the procedure for forming plasma-treated, highly oxidation-resistant AgNW electrodes. The distance between the substrate and the spray gun was fixed at 20 cm. The density and uniformity of the AgNWs on the glass substrate were controlled by the number of spray cycles used to deposit the AgNWs and by measuring

the optical transmittance of the AgNW-coated glass substrate. The sheet resistance of the sprayed AgNW networks on the glass substrates was maintained at ~20 Ω sq^{-1} and their optical transmittance was ~80% at 550 nm. The AgNW networks on the glass substrate were then plasma-treated to form C_xF_y polymers with a 60 MHz (VHF) capacitively coupled plasma (CCP) system operating with a constant power of 150 W. The polymerization gases, c-C_4F_8 (octafluorocyclobutane-fluorocarbon molecules with circular structure) and 1,3-C_4F_6 (hexafluoro-1,3-butadiene-fluorocarbon molecules with straight chain structure), were used at gas flow rates of 80 sccm, an operating pressure of 30 mTorr, and at a temperature of 20 °C.

The AgNWs will be slowly oxidized by oxygen and moisture in the natural atmosphere; therefore, a series of aging experiments were carried out in environmental conditions expected to accelerate the oxidation process (80% humidity and 20 °C). The samples were exposed to these accelerating conditions for a period of up to 36 d.

To evaluate their electrochemical stability, the sheet resistances of the 25 mm × 25 mm AgNW samples were measured periodically with a 4-point probe (CMT-SR2000N) every 3 d. The optical transmittance was measured with an ultraviolet–visible spectrophotometer (UV-3600 Shimadzu) after the baseline for the spectroscopy was set by scanning a clean glass substrate. The haze values were measured with a haze meter (BYK-Gardner haze-gard i). The plasma-treated AgNWs were examined by field emission scanning electron microscopy (SEM, S-4700 Hitachi). The surface morphologies and root mean square roughness of the pristine and plasma-treated AgNWs were measured by atomic force microscopy (AFM, E-sweep Nano Navi) in the tapping mode. In order to investigate the adhesion of the plasma-treated AgNWs, a piece of 3 M scotch magic tape was attached to the AgNW samples and detached. After the plasma processing, the composition and chemical binding states of the fluorocarbon polymer layer were investigated by x-ray photoelectron spectroscopy (XPS, ESCA2000 VG Microtech Inc.), and narrow scans of the C 1 s, O 1 s, and Ag 3 s binding states were obtained after treatments with a C_4F_8 plasma and a C_4F_6 plasma. The structure of the plasma-treated AgNWs was determined by x-ray diffraction (XRD, D8 ADVANCE Bruker Corp). The modification of AgNW surfaces by the plasmas was investigated by Fourier transform infrared (FT-IR, ALPHA Bruker Corp) spectroscopy; infrared spectra were obtained between 4000 and 400 cm^{-1} in the attenuated total reflection mode. A quadrupole mass spectrometer (QMS, PSM003 Hiden analytical Ltd) attached to a chamber wall was used to investigate dissociated species of C_xF_y from the C_4F_8 and C_4F_6 plasmas. The water contact angles of the AgNWs before and after coating with fluorocarbon plasmas were measured using a contact angle analyzer (Phoenix 450 SEO).

3. Results and discussion

To passivate the AgNWs, the AgNW electrodes formed on glass substrates were exposed to fluorocarbon plasmas of C_4F_8 (80 sccm) or C_4F_6 (80 sccm) at 30 mTorr and with a 60 MHz (VHF) power source. The plasma system and a schematic drawing of the surface treatment with dissociated C_xF_y radicals are shown in figure S1 is available online at stacks.iop.org/NANO/0/000000/mmedia (online supplementary information). The effect of RF power (at a fixed treatment time of 30 s) and surface treatment time (at an RF power of 150 W) on the optical transmittance at 550 nm (black), haziness (blue), and sheet resistance (red) of the surface-treated AgNW electrode are shown in figures 2(a) and (b), respectively. As shown in figure 2(a), at an RF power of 150 W, the optical transmittance values measured at 550 nm were similar to that of the reference sample. However, increasing the RF power to 350 W slightly decreased the optical transmittance from ~80% to ~75% for both C_4F_6 and C_4F_8. The haziness and sheet resistance were also similar to those of the reference sample at an RF power of 150 W; however, increasing the RF power to 350 W increased the sheet resistance from ~9 to ~10.5 Ω/sq for both C_4F_6 and C_4F_8-treated samples and increased the haziness slightly from ~1.2% to ~1.5% for C_4F_8 and significantly to ~2.1% for C_4F_6. When the surface treatment time was varied from 15 to 90 s while keeping the RF power at 150 W, as shown in figure 2(b), the optical transmittance measured at 550 nm, sheet resistance, and haziness were similar to those of the reference sample until 60 s. However, when the surface treatment time was further increased to 90 s, those values significantly varied from ~80% to ~70% for optical transmittance, from ~1.2% to ~2.5% for haziness, and from ~9 to ~12 Ω/sq for sheet resistance, similarly for the C_4F_6 and C_4F_8-treated samples. When C_4F_6 and C_4F_8 were compared, the C_4F_8-treated AgNWs generally showed a higher optical transmittance, lower haziness, and lower sheet resistance compared to the C_4F_6-treated AgNWs at the same treatment time. Furthermore, an RF power of 150 W and treatment time of 30 s were identified as the optimal surface treatment conditions.

Figures 2(c) and (d) show the optical transmittance spectra for the wavelength range from 400 to 1000 nm and optical pictures of AgNWs/glass substrates before and after surface treatment with C_4F_8 and C_4F_6, respectively. The AgNWs/glass substrates were surface-treated at an RF power of 150 W for 30 s. As shown in figure 2(c), even though the optical transmittance values at 550 nm were similar for C_4F_8 and C_4F_6, the C_4F_6-treated AgNW/glass substrate showed a lower transmittance at shorter wavelengths and a higher transmittance at longer wavelengths after the surface treatment and, therefore, showed a slightly yellowish color compared to the untreated AgNWs/glass substrate, as shown in figure 2(d). In the case of C_4F_8, the optical transmittance spectrum and color of the C_4F_8-treated AgNWs/glass substrate were similar to those of the untreated AgNWs/glass substrate.

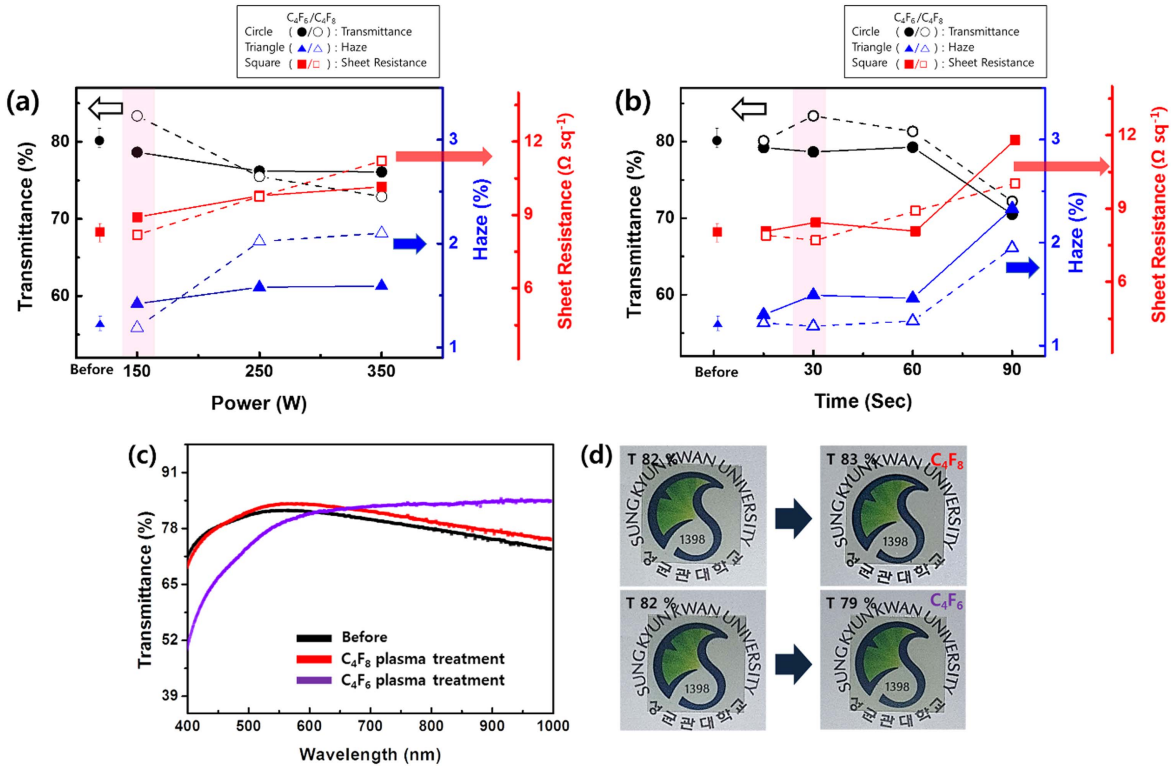

Figure 2. AgNWs before and after the C_4F_8 and C_4F_6 plasma treatments. Haziness, sheet resistance, and optical transmittance of plasma-treated AgNWs on glass substrates as a function of (a) plasma source RF power for 30 s of plasma treatment time and (b) the plasma treatment time for 150 W of RF power. (c) Optical transmittance of AgNWs/glass substrate measured as a function of wavelength for AgNWs/glass substrate treated with C_4F_6 plasma and C_4F_8 plasma for 30 s. (d) Optical images of AgNWs/glass substrates before and after the treatment with C_4F_6 plasma and C_4F_8 plasma for 30 s.

To investigate the differences between the C_4F_8 and C_4F_6 surface treatments, the AgNW electrodes treated with C_4F_8 and C_4F_6 for different times up to 120 s were examined using SEM and the results are shown in figures 3(a)–(d) for C_4F_8 and figures 3(e)–(h) for C_4F_6. As shown in figures 3(a)–(d), the morphology of the AgNWs did not change significantly even though the AgNWs were treated with C_4F_8 plasma for 120 s. However, as shown in figures 3(e)–(h), the thickness of the AgNWs treated with C_4F_6 increased significantly with increasing treatment time, even after a treatment time of 15 s.

Cross-sections of the AgNWs treated with C_4F_8 and C_4F_6 for 30 s at 150 W were observed using SEM and the results are shown in figures 4(a) and (b), respectively. As shown in figures 4(a) and (b), in the case of C_4F_8, the polymer layer uniformly covered the AgNWs and glass substrate like a blanket; and, the size of the AgNWs did not increase significantly with increasing treatment time. On the contrary, in the case of C_4F_6, the polymer grew around the AgNWs, therefore, the diameter of the AgNWs was significantly increased with increasing treatment time. Figures 4(c) and (d) show AFM images of the same locations before and after the surface treatment for 30 s at 150 W for C_4F_8 and C_4F_6, respectively. As shown in the images, no significant change in the diameter of the AgNWs was observed for C_4F_8 while significant changes in the diameter of the AgNWs were observed for C_4F_6 at the same locations, similar to the SEM images shown in figure 3.

For plasmas using fluorocarbon gases such as C_4F_8 and C_4F_6, the C/F ratio in the gas molecule determines the deposition rate of the fluorocarbon layer on the material surface. When the fluorocarbon gas has a higher C/F ratio, a thicker polymer layer is formed on the material surface. C_4F_6-based gas tends to generate more high-molecular weight radicals that act as polymer-rich precursors in the plasma compared to C_4F_8-based gas, due to a higher C/F ratio [40–42]. Therefore, the C_4F_6 plasma tends to form a thicker polymer layer on the AgNW/glass substrate compared to the C_4F_8 plasma due to the higher C/F ratio. However, even though the polymer layer is thin, a uniform blanket-type deposition of the polymer layer is observed for C_4F_8, while a thicker and more specific growth of a polymer layer around the AgNW surface is shown for C_4F_6, in figures 4(e) and (f), respectively. The differences in the morphology of the deposited fluorocarbons on AgNWs are believed to be due to the differences in the growth mechanism of the polymer layer on AgNW between the C_4F_8 plasma and C_4F_6 plasma.

To investigate the possible differences in the growth mechanisms of the polymer layer on AgNWs for C_4F_8 plasma and C_4F_6 plasma, the AgNWs treated with C_4F_6 and C_4F_8 for 30 s were analyzed with XRD and XPS. Figure 5(a) shows the XRD patterns of AgNWs before and after the treatment with C_4F_8 plasma and C_4F_6 plasma. As shown in the figures, intensity peaks related to the (111), (200), (220), and (311) planes could be identified at $2\theta = 38.1°$, 44.3°, 64.5°, and

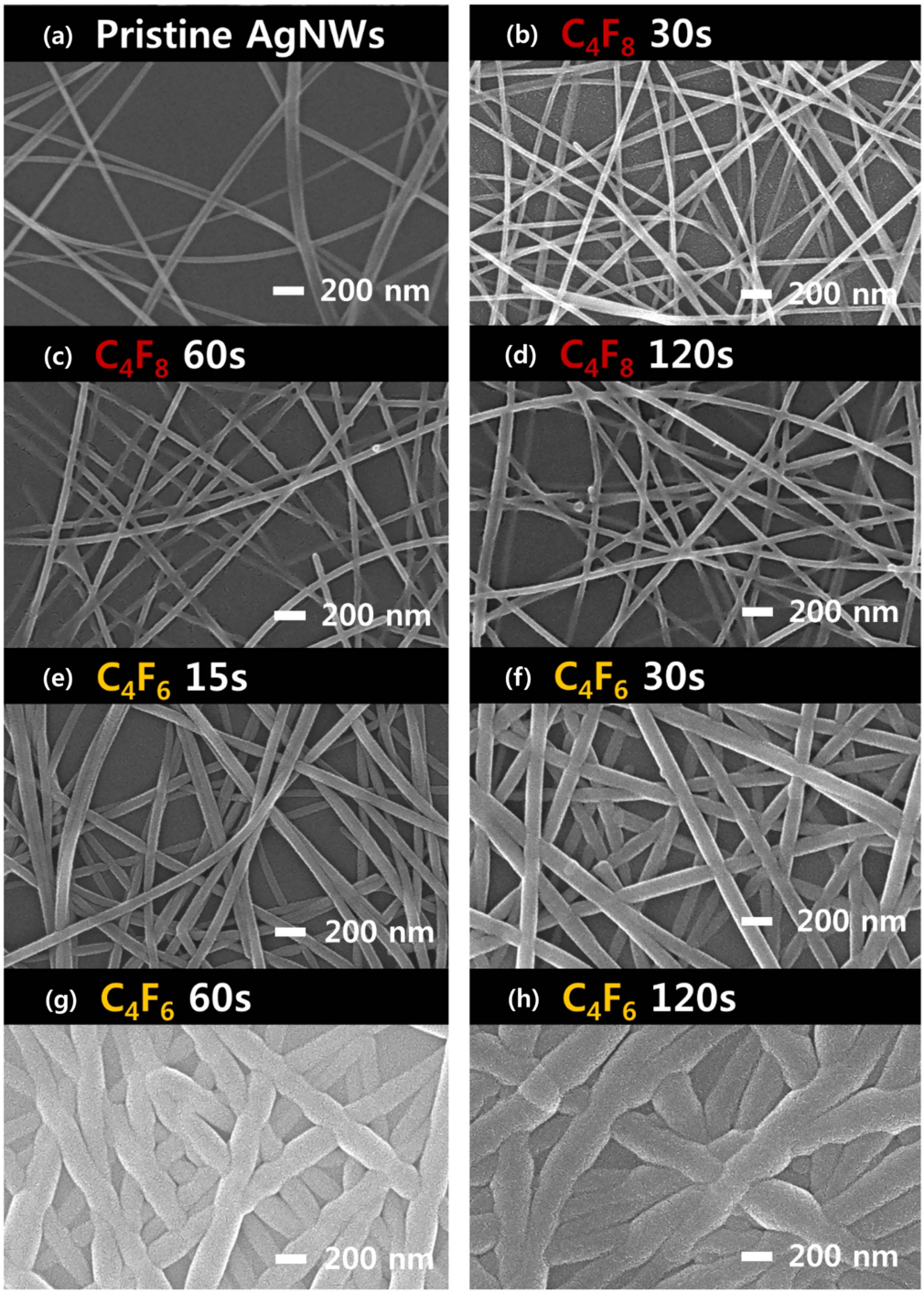

Figure 3. SEM images of AgNWs before and after the plasma treatments with C_4F_6 plasmas and C_4F_8 plasmas. (a) Pristine AgNWs, and AgNWs treated with C_4F_8 plasma for (b) 30 s, (c) 60 s, and (d) 120 s. AgNWs treated with C_4F_6 plasma for (e) 15 s, (f) 30 s, (g) 60 s, and (h) 120 s.

77.4°, respectively, based on the Joint Committee on Powder Diffraction Standards, but no differences in signal intensities were observed before and after the plasma treatments, indicating no change in the AgNW structure after the plasma treatments. Figures 5(b)–(e) show XPS narrow scan data of the Ag 3d, C 1s, O 1s, and F 1s peaks, respectively, before and after the plasma treatments. The XPS survey spectra and atomic composition of C, F, O, and Ag on the surfaces of AgNWs before and after the plasma treatments are shown in figure S2 (online supplementary information). Two peaks in the Ag 3d spectra located at 368.2 and 374.3 eV in figure 5(b) are related to the electron binding energies from the Ag $3d_{5/2}$ and Ag $3d_{3/2}$ orbitals, respectively. After the plasma treatments, the Ag binding peak intensities were decreased for both C_4F_8 and C_4F_6, but more significantly for the C_4F_6 plasma-treated AgNWs due to the thicker polymer layer formed around the AgNWs. As shown in figures 5(d) and (e), due to the formation of a fluorocarbon polymer layer on the

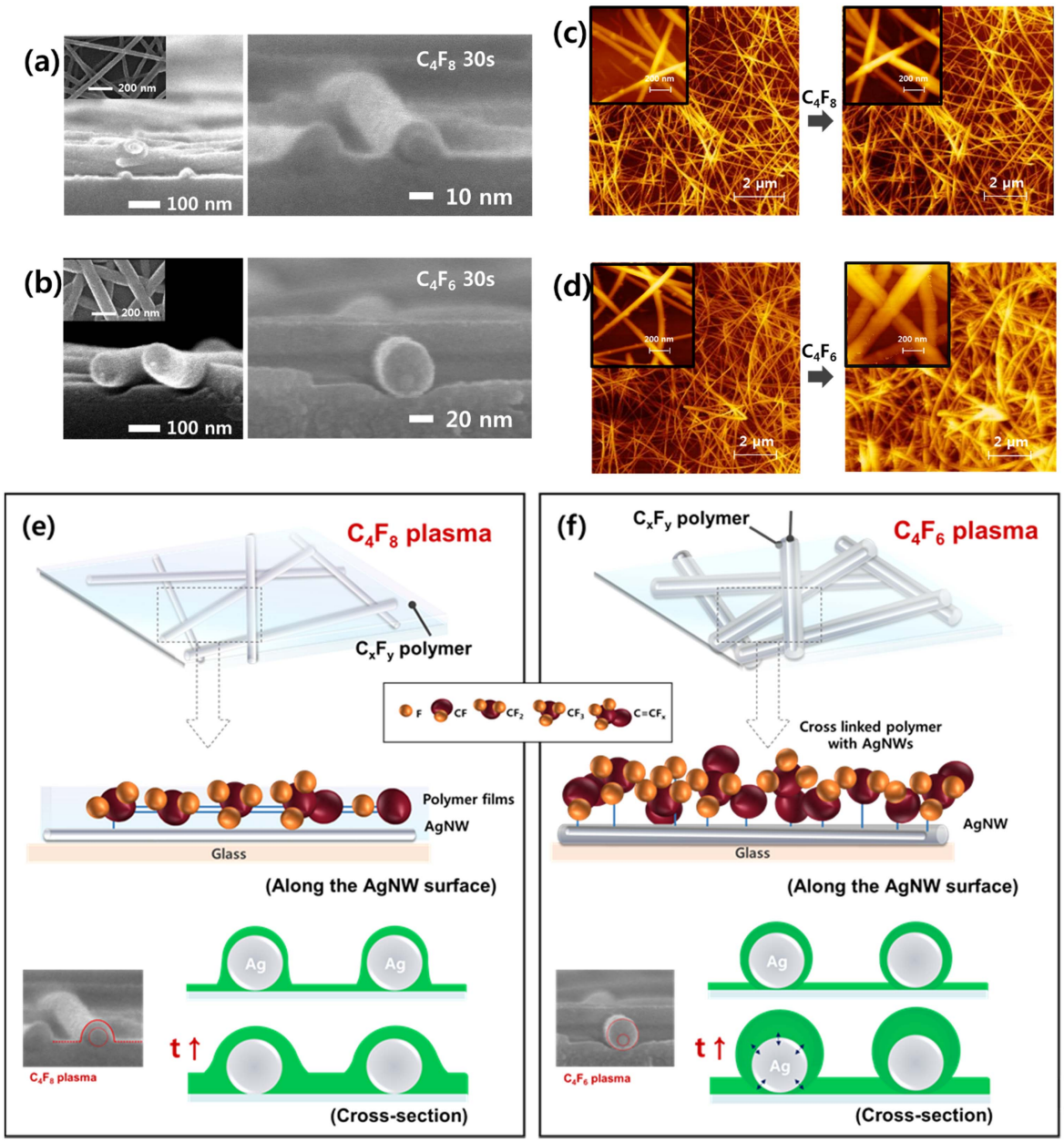

Figure 4. Cross-sectional SEM images of AgNWs after the plasma treatment with (a) C_4F_8 for 30 s and (b) C_4F_6 for 30 s. Planar SEM images of AgNWs are also shown in the inset. AFM images of AgNWs after the plasma treatment with (c) C_4F_8 for 30 s and (d) C_4F_6 for 30 s. Cartoons of the possible fluorocarbon formation mechanism on AgNW surface for (e) C_4F_8 plasma and (f) C_4F_6 plasma.

AgNWs, C–F binding peaks and fluorine peaks were observed after the plasma treatments with C_4F_8 and C_4F_6. Compared to the C_4F_8 plasma-treated AgNWs, the C_4F_6 plasma-treated AgNWs showed a more dominant binding peak related to C–F/C=O in the C 1s spectra, as shown in figure 5(d). Especially in the case of the oxygen binding peaks shown in figure 5(c), binding peaks related to metal carbonates/C–O and C=O were also observed for the C_4F_6 plasma-treated AgNWs, while no such peaks were observed for pristine AgNWs or C_4F_8 plasma-treated AgNWs. In the case of the Ag binding peaks, due to the small differences between the binding energies of Ag $3d_{5/2}$ for oxides/carbonates, that is, Ag (368.2 eV), AgO (367.6 eV), Ag_2O (367.9 eV), and Ag_2CO_3 (367.7 eV), the existence of oxide and metal carbonates could not be determined.

The formation of C=O bonds in the C_4F_6 plasma-treated AgNWs could be also identified using FT-IR spectroscopy. As shown in figure 5(f), both C_4F_6 and C_4F_8 plasma-treated AgNWs showed absorption peaks related to CF_x (1000–1350 cm^{-1}) and COF_2 (774 and 1944 cm^{-1}). However, the C_4F_6 plasma-treated AgNWs showed an additional C=O absorption peak (1730 cm^{-1}) as well as a higher CF_x absorption peak. (The differences of FT-IR data between C_4F_8 and C_4F_6 plasmas could be also from the thickness differences between the polymer thickness deposited by C_4F_8 plasma and C_4F_6 plasma. However as shown in figure 5(f), the FT-IR data observed for C_4F_8 plasma-treated AgNWs for

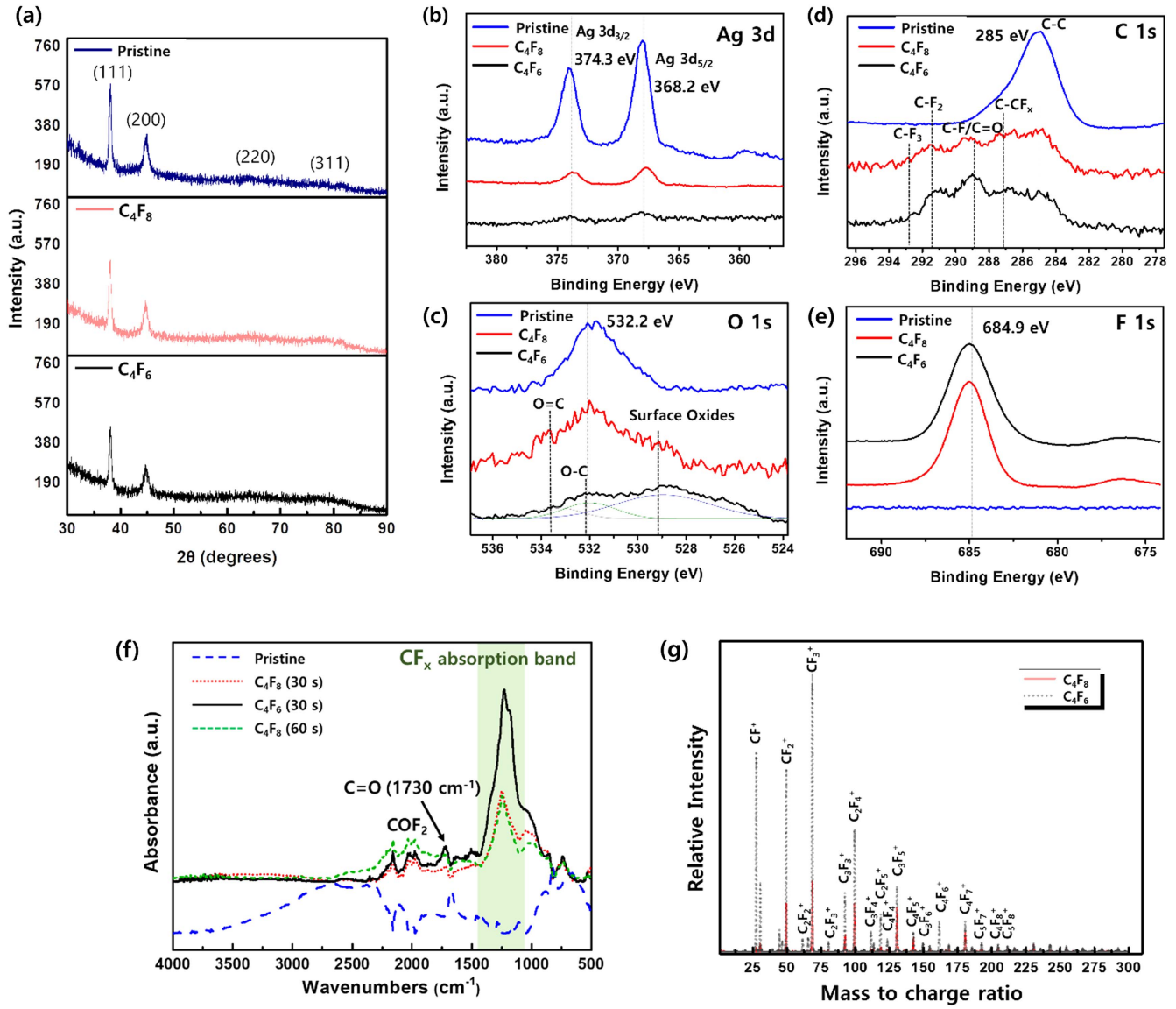

Figure 5. (a) XRD patterns of AgNWs before and after the plasma treatment with C_4F_8 and C_4F_6 for 30 s. XP spectra of AgNWs before and after the plasma treatment with C_4F_8 and C_4F_6 for 30 s; (b) Ag 3d, (c) O 1s, (d) C 1s, and (e) F 1s. (f) FT-IR spectra of AgNWs before and after the plasma treatment with C_4F_8 and C_4F_6 for 30 s. (g) QMS data measured for C_4F_8 and C_4F_6 plasma at an RF power of 150 W.

60 s also showed the similar trend as those treated for 30 s, therefore, the differences of FT-IR data between C_4F_8 plasma and C_4F_6 plasma were not related to the polymer thickness.) The C–O/C=O bonds observed by XPS and FT-IR for the C_4F_6 plasma-treated AgNWs indicate stronger binding of the AgNWs with fluorocarbon radicals from the C_4F_6 plasma (that is, the binding of oxygen on the AgNW surface with carbon in the fluorocarbon radicals from the C_4F_6 plasma).

The differences in the fluorocarbon radicals generated in the C_4F_8 and C_4F_6 plasmas were observed using QMS and the results are shown in figure 5(g). As shown in figure 5(g), the C_4F_6 plasma contains more highly reactive fluorocarbon radicals such as CF, CF_2, and CF_3 compared to the C_4F_8 plasma. Therefore, it is believed that due to the presence of more and highly reactive radicals in the C_4F_6 plasma, a thick fluorocarbon polymer layer grows around the AgNWs with strong chemical bonds between the fluorocarbon radicals and the AgNW surface, while the C_4F_8 plasma forms a thin and uniform blanket-type polymer layer on the AgNW/glass substrate surface [43–46].

Using the AgNW/glass substrates treated by C_4F_6 and C_4F_8 plasmas for 0–30 s with 150 W of RF power, the resistivity change of the AgNWs by oxidation was investigated. For oxidation tests, the AgNWs were placed in a harsh environment (temperature of 20 °C and humidity of 80%). The change in the AgNW sheet resistance was measured every 3 for 36 d and the results are shown in figures 6(a) and (b). As shown in figure 6(a), the resistance of the pristine AgNWs increased significantly (an increase of ~176.2 times) after 36 d in the harsh environment due to the oxidation of the AgNWs. However, after the plasma treatments, the increase in the resistance of the AgNWs was smaller due to the fluorocarbon polymer layer on the AgNW surface, which protected the AgNW surface from the harsh environment.

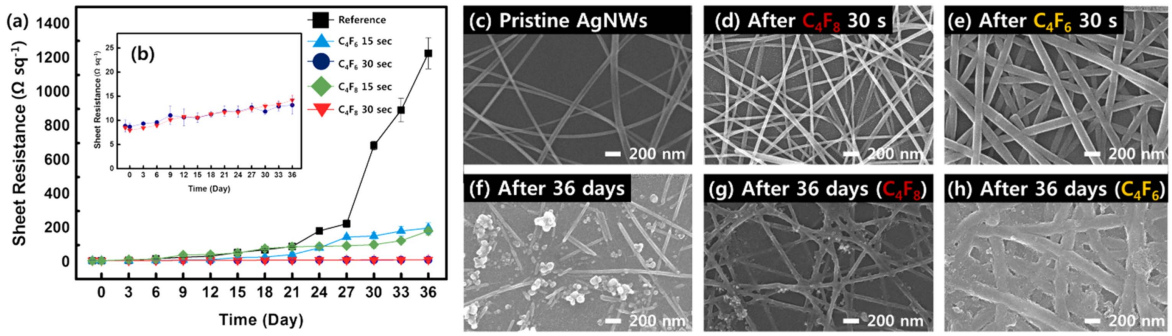

Figure 6. (a) and (b) Oxidation stability of pristine AgNWs and the AgNWs treated with C_4F_8 and C_4F_6 plasmas in accelerating environmental conditions (humidity 80% and 20 °C) to speed up the oxidation. SEM images of AgNWs (c) pristine, (d) after 30 s of C_4F_8 plasma treatment, (e) after 30 s of C_4F_6 plasma treatment. (f)–(h) Show SEM images of the AgNWs in (c)–(e), respectively, after exposure for 36 d under 80% humidity and 20 °C.

Particularly, when the plasma treatment time was 30 s, no significant change in the AgNW sheet resistance (an increase of ∼1.6 times) after 36 d was observed, as shown in figure 6(b). This is possibly due to the encapsulation effect for both AgNW/glass substrates treated by C_4F_6 and C_4F_8. When the pristine AgNWs and those treated with C_4F_6 and C_4F_8 plasmas for 30 s were observed by SEM after 36 d in the harsh environment, the pristine AgNWs showed broken AgNW junctions due to oxidation as shown in figures 6(c) and (f), while the AgNWs treated with C_4F_6 and C_4F_8 plasmas for 30 s showed NW junctions that remained unbroken as shown in figures 6(d) and (g) for C_4F_8 and figures 6(e) and (h) for C_4F_6. For the AgNWs treated with the C_4F_6 plasma or the C_4F_8 plasma, even though some corrosion was observed on the AgNW surfaces, the AgNW junctions were preserved due to the protection of the AgNW surfaces by the fluorocarbon polymer layer. Therefore, even though the plasma treatment conditions and properties of the deposited polymer layers were different, sufficient oxidation protection of the AgNWs could be achieved for both C_4F_8 and C_4F_6 plasmas by treating for 30 s.

For the AgNW/glass substrates, before and after the plasma treatments with C_4F_6 and C_4F_8 for 30 s, the degree of adhesion was investigated using the 3 M tape peel-off and the results are shown in figures 7(a)–(c) for pristine AgNWs, C_4F_6 plasma-treated AgNWs, and C_4F_8 plasma-treated AgNWs, respectively, (the left side shows SEM images after peel-off, right side shows AgNWs as-is). For the AgNW peel-off test, 3 M tape was attached firmly on the AgNW/glass substrates, including those treated with C_4F_6 plasma and C_4F_8 plasma. The 3 M tape was then peeled-off with tweezers at an angle of ∼180°. As shown in the figures, in the case of pristine AgNWs, the AgNWs were easily detached from the substrate by the peel-off test, whereas the plasma-treated samples remained almost intact, indicating stronger adhesion to the glass substrate after the plasma treatments. Therefore, after the plasma treatments with C_4F_6 and C_4F_8 for 30 s, improved adhesion of AgNWs on the glass substrate could be achieved in addition to the improved oxidation resistance. In fact, one may think that better adhesion result obtained with C_xF_y coated AgNWs compared to AgNWs itself may not be from the improved adhesion of AgNWs to substrate by the C_xF_y polymer but from the antiadhesive behavior of C_xF_y polymer such as Teflon to the Scotch tape during the Scotch tape test (see figure S3, online supplementary information). However, even if the C_xF_y polymers do not have significant adhesion strength to the AgNWs and the substrate, the Scotch tape test showed no peeling-off for the AgNWs coated with C_xF_y indicating that the AgNWs stayed on the substrate due to the C_xF_y coating. Therefore, compared to the adhesion of AgNWs to the substrate itself, the adhesion of C_xF_y to AgNWs and the substrate was higher and, eventually, improved adhesion of AgNWs to the substrate.

When the electrical, optical, chemical, and mechanical characteristics are considered, AgNWs treated with C_4F_8 plasma at the optimized conditions of 150 W of RF power and 30 s of surface treatment time showed better characteristics due to their lower sheet resistance, higher optical transmittance, and lower haziness compared to C_4F_6-treated AgNWs, while AgNWs treated with either plasma showed similar corrosion protection and adhesion characteristics.

4. Conclusions

In conclusion, oxidation-resistant hybrid AgNWs were fabricated without sacrificing their transparency and sheet resistance using C_4F_8 or C_4F_6 plasma treatments. Increasing the plasma treatment time up to 60 s (the optimized time was 30 s) with 150 W of RF power did not significantly change the sheet resistance, haziness, or optical transmittance of the AgNWs, while further increases in the plasma treatment time did increase the sheet resistance/haziness and decreased the optical transmittance significantly. The fluorocarbon polymer layer on the AgNWs treated by a C_4F_6 plasma was thicker and formed around the AgNWs, while a thin and uniform blanket-type fluorocarbon polymer layer was formed on the AgNW/glass substrate surface by the C_4F_8 plasma. However, the oxidation resistance after the plasma treatment for 30 s was similar and sufficiently high for both C_4F_6 and C_4F_8 plasmas, regardless of the characteristics of the polymer formed on the AgNWs. No significant oxidation was observed after exposure to a harsh environment for 36 d while the adhesion to the substrate was also improved. However,

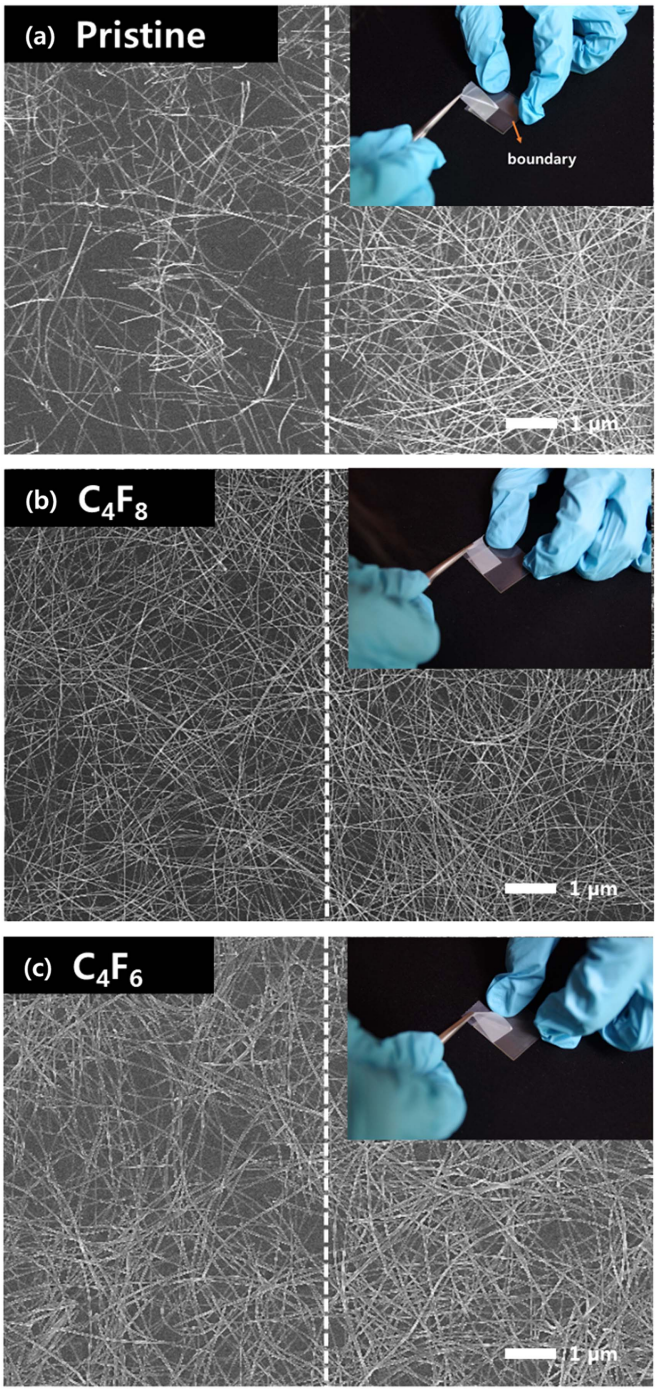

Figure 7. SEM images of AgNWs after tape test (left) and before (right); (a) pristine AgNWs, (b) C_4F_6 plasma-treated AgNWs, and (c) C_4F_8 plasma-treated AgNWs. Inserts show photograph of the scotch tape test for AgNWs on glass substrates treated/untreated with the plasmas. A piece of scotch tape was firmly attached on the AgNW surfaces and then rapidly detached.

when all the characteristics are considered, the C_4F_8 plasma-treated AgNWs exhibited better characteristics compared to the C_4F_6-treated AgNWs due to their lower sheet resistance, higher optical transmittance, and lower haziness. It is believed that various NWs including AgNWs and CuNWs can be easily protected from oxidizing environments by the plasma treatment investigated in this study because large-area fluorocarbon plasmas can be easily generated using CCP equipment.

Acknowledgments

This study was supported by the National Research Foundation of Korea (NRF-2016M3A7B4910429).

ORCID iDs

Geun Young Yeom https://orcid.org/0000-0001-6603-2193

References

[1] Hu L, Kim H S, Lee J-Y, Peumans P and Cui Y 2010 Scalable coating and properties of transparent, flexible, silver nanowire electrodes *ACS Nano* **4** 2955
[2] Wu H, Hu L, Rowell M W, Kong D, Cha J J, McDonough J R, Zhu J, Yang Y, McGehee M D and Cui Y 2010 Electrospun metal nanofiber webs as high-performance transparent electrode *Nano Lett.* **10** 4242
[3] Rathmell A R, Nguyen M, Chi M and Wiley B J 2012 Synthesis of oxidation-resistant cupronickel nanowires for transparent conducting nanowire networks *Nano Lett.* **12** 3193
[4] Kim S, Kim S Y, Chung M H, Kim J and Kim J H 2015 A one-step roll-to-roll process of stable AgNW/PEDOT: PSS solution using imidazole as a mild base for highly conductive and transparent films: optimizations and mechanisms *J. Mater. Chem.* C **3** 5859
[5] Won Y, Kim A, Lee D, Yang W, Woo K, Jeong S and Moon J 2014 Annealing-free fabrication of highly oxidation-resistive copper nanowire composite conductors for photovoltaics *NPG Asia Mater.* **6** e105
[6] Liu C-H and Yu X 2011 Silver nanowire-based transparent, flexible, and conductive thin *film Nanoscale Res. Lett.* **6** 75
[7] Ye S, Rathmell A R, Chen Z, Stewart I E and Wiley B J 2014 Metal nanowire networks: the next generation of transparent conductors *Adv. Mater.* **26** 6670
[8] Kim A, Won Y, Woo K, Jeong S and Moon J 2014 All-solution-processed indium-free transparent composite electrodes based on Ag nanowire and metal oxide for thin-film solar cells *Adv. Funct. Mater.* **24** 2462
[9] Langley D, Giusti G, Mayousse C, Celle C, Bellet D and Simonato J-P 2013 Flexible transparent conductive materials based on silver nanowire networks: a review *Nanotechnology* **24** 452001
[10] Menamparambath M M, Ajmal C M, Kim K H, Yang D, Roh J, Park H C, Kwak C, Choi J-Y and Baik S 2015 Silver nanowires decorated with silver nanoparticles for low-haze flexible transparent conductive films *Sci. Rep.* **5** 16371
[11] Kholmanov I N, Domingues S H, Chou H, Wang X, Tan C, Kim J-Y, Li H, Piner R, Zarbin A J and Ruoff R S 2013 Reduced graphene oxide/copper nanowire hybrid films as high-performance transparent electrodes *ACS Nano* **7** 1811
[12] Song J, Li J, Xu J and Zeng H 2014 Superstable transparent conductive Cu@Cu_4Ni nanowire elastomer composites against oxidation, bending, stretching, and twisting for flexible and stretchable optoelectronics *Nano Lett.* **14** 6298
[13] Huang G-W, Xiao H-M and Fu S-Y 2014 Based silver-nanowire electronic circuits with outstanding electrical

conductivity and extreme bending stability *Nanoscale* **6** 8495
[14] Im H-G, Jung S-H, Jin J, Lee D, Lee J, Lee D, Lee J-Y, Kim I-D and Bae B-S 2014 Flexible transparent conducting hybrid film using a surface-embedded copper nanowire network: a highly oxidation-resistant copper nanowire electrode for flexible optoelectronics *ACS Nano* **8** 10973
[15] Yin Z, Lee C, Cho S, Yoo J, Piao Y and Kim Y S 2014 Facile synthesis of oxidation-resistant copper nanowires toward solution-processable, flexible, foldable, and free-standing electrodes *Small* **10** 5047
[16] Deng B, Hsu P-C, Chen G, Chandrashekar B, Liao L, Ayitimuda Z, Wu J, Guo Y, Lin L and Zhou Y 2015 Roll-to-roll encapsulation of metal nanowires between graphene and plastic substrate for high-performance flexible transparent electrodes *Nano Lett.* **15** 4206
[17] Khaligh H H and Goldthorpe I A 2013 Failure of silver nanowire transparent electrodes under current flow *Nanoscale Res. Lett.* **8** 235
[18] Ahn Y, Jeong Y and Lee Y 2012 Improved thermal oxidation stability of solution-processable silver nanowire transparent electrode by reduced graphene oxide *ACS Appl. Mater. Interfaces* **4** 6410
[19] Jin J, Lee J, Jeong S, Yang S, Ko J-H, Im H-G, Baek S-W, Lee J-Y and Bae B-S 2013 High-performance hybrid plastic films: a robust electrode platform for thin-film optoelectronics *Energy Environ. Sci.* **6** 1811
[20] Elechiguerra J L, Reyes-Gasga J and Yacaman M J 2006 The role of twinning in shape evolution of anisotropic noble metal nanostructures *J. Mater. Chem.* **16** 3906
[21] Kim A, Won Y, Woo K, Kim C-H and Moon J 2013 Highly transparent low resistance ZnO/Ag nanowire/ZnO composite electrode for thin film solar cells *ACS Nano* **7** 1081
[22] Mayousse C, Celle C, Fraczkiewicz A and Simonato J-P 2015 Stability of silver nanowire based electrodes under environmental and electrical stresses *Nanoscale* **7** 2107
[23] Lee H J, Hwang J H, Choi K B, Jung S-G, Kim K N, Shim Y S, Park C H, Park Y W and Ju B-K 2013 Effective indium-doped zinc oxide buffer layer on silver nanowires for electrically highly stable, flexible, transparent, and conductive composite electrodes *ACS Appl. Mater. Interfaces* **5** 10397
[24] Kim T, Canlier A, Cho C, Rozyyev V, Lee J-Y and Han S M 2014 Highly transparent Au-coated Ag nanowire transparent electrode with reduction in haze *ACS Appl. Mater. Interfaces* **6** 13527
[25] Liu B-T and Huang S-X 2014 Transparent conductive silver nanowire electrodes with high resistance to oxidation and thermal shock *RSC Adv.* **4** 59226
[26] Lee H, Hong S, Lee J, Suh Y D, Kwon J, Moon H, Kim H, Yeo J and Ko S H 2016 Highly stretchable and transparent supercapacitor by Ag–Au core–shell nanowire network with high electrochemical stability *ACS Appl. Mater. Interfaces* **8** 15449
[27] Kim I, Kim Y, Woo K, Ryu E-H, Yon K-Y, Cao G and Moon J 2013 Synthesis of oxidation-resistant core–shell copper nanoparticles *RSC Adv.* **3** 15169
[28] Song T-B, Rim Y S, Liu F, Bob B, Ye S, Hsieh Y-T and Yang Y 2015 Highly robust silver nanowire network for transparent electrode *ACS Appl. Mater. Interfaces* **7** 24601
[29] Xu Q, Shen W, Huang Q, Yang Y, Tan R, Zhu K, Dai N and Song W 2014 Flexible transparent conductive films on PET substrates with an AZO/AgNW/AZO sandwich *structure J. Mater. Chem.* C **2** 3750
[30] Göbelt M, Keding R, Schmitt S W, Hoffmann B, Jäckle S, Latzel M, Radmilović V V, Radmilović V R, Spiecker E and Christiansen S 2015 Encapsulation of silver nanowire networks by atomic layer deposition for indium-free transparent electrodes *Nano Energy* **16** 196
[31] Chen D, Liang J J, Liu C, Saldanha G, Zhao F C, Tong K, Liu J and Pei Q B 2015 Thermally stable silver nanowire-polyimide transparent electrode based on atomic layer deposition of zinc oxide on silver nanowires *Adv. Funct. Mater.* **25** 7512
[32] Meenakshi P, Karthick R, Selvaraj M and Ramu S 2014 Investigations on reduced graphene oxide film embedded with silver nanowire as a transparent conducting electrode *Sol. Energy Mater. Sol. Cells* **128** 264
[33] Im H G, Jin J, Ko J H, Lee J, Lee J Y and Bae B S 2014 Flexible transparent conducting composite films using a monolithically embedded AgNW electrode with robust performance stability *Nanoscale* **6** 711
[34] Cao J and Matsoukas T 2005 Nanowire coating by plasma processing *IEEE Trans. Plasma Sci.* **33** 829
[35] Zhu Y W *et al* 2006 Enhanced field emission from O_2 and CF_4 plasma-treated CuO nanowires *Chem. Phys. Lett.* **419** 458
[36] Li J, Tao Y, Chen S F, Li H Y, Chen P, Wei M Z, Wang H, Li K, Mazzeo M and Duan Y 2017 A flexible plasma-treated silver-nanowire electrode for organic light-emitting devices *Sci. Rep.* **7** 9
[37] Watanabe H and Shimogaki Y 2006 Preparation and characterization of amorphous fluorinated carbon film using low-global-warming-potential gas, C_4F_6, by plasma-enhanced chemical vapor deposition *Japan. J. Appl. Phys.* **45** 8624
[38] Shi D, Lian J, He P, Wang L M, Ooij W J, Schulz M, Liu Y and Mast D B 2002 Plasma deposition of ultrathin polymer films on carbon nanotubes *Appl. Phys. Lett.* **81** 5216
[39] Hung L S, Zheng L R and Mason M G 2001 Anode modification in organic light-emitting diodes by low-frequency plasma polymerization of CHF_3 *Appl. Phys. Lett.* **78** 673
[40] Chinzei Y, Feurprier Y, Ozawa M, Kikuchi T, Horioka K, Ichiki T and Horiike Y 2000 High aspect ratio SiO_2 etching with high resist selectivity improved by addition of organosilane to tetrafluoroethyl trifluoromethyl ether *J. Vac. Sci. Technol.* A **18** 158
[41] Ohya Y, Tomura M, Ishikawa K, Sekine M and Hori M 2016 Formation of a SiOF reaction intermixing layer on SiO_2 etching using $C_4F_6/O_2/Ar$ plasmas *J. Vac. Sci. Technol.* A **34** 040602
[42] Kim J K, Lee S H, Cho S I and Yeom G Y 2015 Study on contact distortion during high aspect ratio contact SiO_2 etching *J. Vac. Sci. Technol.* A **33** 021303
[43] Ushakov A, Volynets V, Jeong S, Sung D, Ihm Y, Woo J and Han M 2008 Study of fluorocarbon plasma in 60 and 100 MHz capacitively coupled discharges using mass spectrometry *J. Vac. Sci. Technol.* A **26** 1198
[44] Cho S W, Kim C K, Lee J K, Moon S H and Chae H 2012 Angular dependences of SiO_2 etch rates in $C_4F_6/O_2/Ar$ and $C_4F_6/CH_2F_2/O_2/Ar$ plasmas *J. Vac. Sci. Technol.* A **30** 051301
[45] Kazumi H, Hamasaki R and Tago K 1995 Model prediction of radical composition in C_4F_8 plasmas and correlation with measured etch characteristics of silicon dioxide *Plasma Sources Sci. Technol.* **5** 200
[46] Benck E C, Goyette A and Wang Y 2003 Ion energy distribution and optical measurements in high-density, inductively coupled C_4F_6 discharges *J. Appl. Phys.* **94** 1382